Bioorganic & Medicinal Chemistry Letters xxx (xxxx) xxx–xxx

Contents lists available at ScienceDirect

Bioorganic & Medicinal Chemistry Letters

journal homepage: www.elsevier.com/locate/bmcl

Optimization of *N*-benzyl-5-nitrofuran-2-carboxamide as an antitubercular agent

Ricardo Gallardo-Macias[a], Pradeep Kumar[b], Mark Jaskowski[a], Todd Richmann[b], Riju Shrestha[b], Riccardo Russo[b], Eric Singleton[b], Matthew D. Zimmerman[c], Hsin Pin Ho[c], Véronique Dartois[c], Nancy Connell[b], David Alland[b], Joel S. Freundlich[a,b,*]

[a] Department of Pharmacology, Physiology, and Neuroscience, Rutgers University – New Jersey Medical School, Newark, NJ, USA
[b] Division of Infectious Disease, Department of Medicine and the Ruy V. Lourenço Center for the Study of Emerging and Re-emerging Pathogens, Rutgers University – New Jersey Medical School, Newark, NJ, USA
[c] Public Health Research Institute, Rutgers University – New Jersey Medical School, Newark, NJ, USA

ARTICLE INFO

Keywords:
Mycobacterium tuberculosis
Nitrofuran
Benzamide
α, α-Dimethyl

ABSTRACT

The optimization campaign for a nitrofuran antitubercular hit (*N*-benzyl-5-nitrofuran-2-carboxamide; **JSF-3449**) led to the design, synthesis, and biological profiling of a family of analogs. These compounds exhibited potent *in vitro* antitubercular activity (MIC = 0.019–0.20 μM) against the *Mycobacterium tuberculosis* H37Rv strain and low *in vitro* cytotoxicity (CC_{50} = 40– > 120 μM) towards Vero cells. Significant improvements in mouse liver microsomal stability and mouse pharmacokinetic profile were realized by introduction of an α, α-dimethylbenzyl moiety. Among these compounds, **JSF-4088** is highlighted due to its *in vitro* antitubercular potency (MIC = 0.019 μM) and Vero cell cytotoxicity (CC_{50} > 120 μM). The findings suggest a rationale for the continued evolution of this promising series of antitubercular small molecules.

Tuberculosis (TB), caused by *Mycobacterium tuberculosis*, is a deadly airborne infectious disease that led to 1.7 million deaths in 2016.[1] It is believed that one-third of the world's population is infected with TB and ca. 10 million new cases have been reported annually. Front-line TB chemotherapy, developed > 50 years ago, includes a 2-month treatment with isoniazid (INH), rifampicin (RIF), pyrazinamide (PZA), and ethambutol (EMB) followed by 4 months of INH and RIF. However, the emergence of multi-drug resistant and extensively-drug resistant TB strains has rendered TB a very challenging infectious disease to treat.[2] Therefore, new chemotherapeutic agents, characterized by a novel mechanism of action, improved efficacy, and potential for significantly shortening the current length of treatment, are required.

Pretomanid,[3] delamanid,[4] and metronidazole,[5] feature a nitroimidazole moiety, and are of clinical relevance as antitubercular agents (Fig. 1). Delamanid was approved in Europe in 2014, while both it and pretomanid are in clinical trials in the United States. In a completed clinical study, metronidazole exhibited some benefit with respect to shortening drug therapy, but neurotoxic adverse events were deemed a critical limitation.[6] It is proposed that the nitro moiety, in both pretomanid and delamanid, undergoes intrabacterial drug metabolism by a deazaflavin-dependent nitroreductase, Ddn.[7] This bioactivation produces nitric oxide (NO•),[8] a reactive nitrogen species (RNS) that has been demonstrated to have cidal consequences for the bacterium.[3] Even though pretomanid and delamanid are novel antitubercular agents with efficacy against both drug-sensitive and drug-resistant TB strains, these investigational drugs suffer from points of weakness. For example, pretomanid and delamanid exhibit a relatively high frequency of resistance (e.g., 10^{-5} – 10^{-6}) coupled with dramatic losses (≥500X) of potency versus such mutants.[9,10]

As an alternative to these nitroimidazoles, nitrofuran containing compounds have also demonstrated antitubercular activity. For instance, nitrofuranylamides, nitrofuranylpiperazines, and nitrofuranylisoxazolines have demonstrated *in vitro* and *in vivo* efficacy (Fig. 2),[11–16] but to the best of our knowledge have yet to transition to clinical studies. Inspired by these compounds and our efforts with distantly related triazine[17] and pyrimidine[18] series, we decided to further probe the structure-activity relationship (SAR) of nitrofuranylamides as antitubercular agents. We commenced with the hit compound **JSF-3449** from our internal screening efforts,[19] and pursued its evolution to an α, α-dimethyl benzylamide **JSF-4088** (Fig. 2). Herein, we discuss how this optimization proceeded, outlining the hurdles that were overcome and those that remain in the pursuit of a candidate for *in vivo*

* Corresponding author at: Department of Pharmacology, Physiology, and Neuroscience, Rutgers University – New Jersey Medical School, Newark, NJ, USA.
E-mail address: freundjs@rutgers.edu (J.S. Freundlich).

https://doi.org/10.1016/j.bmcl.2018.12.053
Received 27 October 2018; Received in revised form 20 December 2018; Accepted 22 December 2018

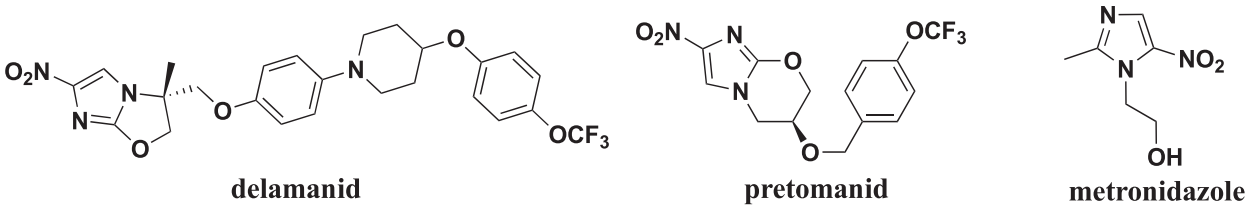

Figure 1. The chemical structures of delamanid, pretomanid, and metronidazole.

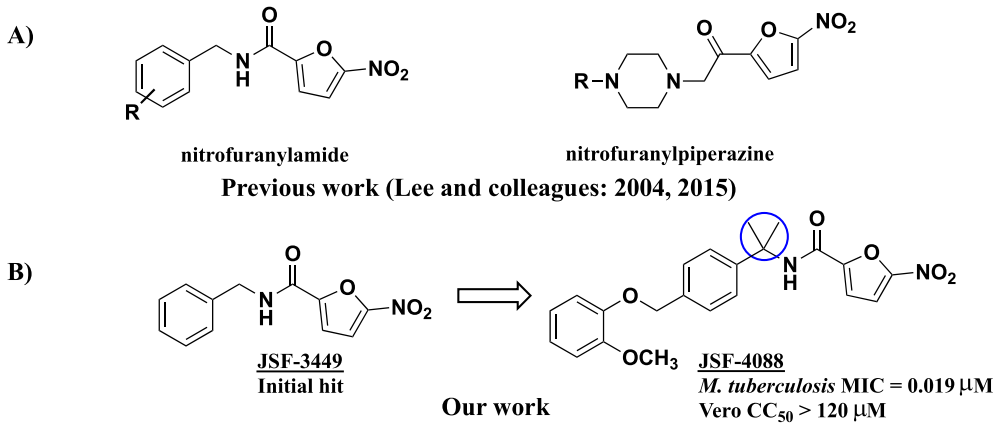

Figure 2. A) Nitrofuranylbenzylamides as antitubercular agents and B) highlight of our introduction of α, α-dimethyl substitution of the benzylic carbon to afford **JSF-4088**.

efficacy studies.

JSF-3449, which appears to have first been noted as displaying antitubercular activity in 1967, [20] exhibited in our hands a modest minimal inhibitory concentration (MIC; minimum concentration of compound that achieves 90% growth inhibition of the *in vitro* cultured bacteria) of 0.39 μM versus the H37Rv laboratory strain of *M. tuberculosis*. A more potent (lower value) MIC was set as an optimization goal. The hit's Vero cell cytotoxicity CC_{50} (minimum compound concentration that inhibits growth of this model mammalian cell line by 50%) was 13 μM. The SI value (CC_{50}/MIC) of 33, acceptable for a hit compound (≥10), was also targeted for improvement by not only a decrease in MIC but also by an increase in CC_{50}.[18] **JSF-3449** was profiled versus a panel of ESKAPE pathogens and was selective for *M. tuberculosis* (Supplemental Information, Table S1). Due to the potency of **JSF-3449**, we further assayed **JSF-3449** for *in vitro* mouse liver microsome (MLM) stability and kinetic solubility (S) in pH 7.4 PBS as well as mouse pharmacokinetic (PK) profile. **JSF-3449** displayed an MLM $t_{1/2}$ = 28.5 min, and S > 500 μM. Ideally, the $t_{1/2}$ would be greater than or equal to 60 min, but the solubility was more than satisfactory (> 100 μM).[18] Oral dosing (po) of **JSF-3449** in CD-1 female mice, at a level of 25 mg/kg in 5% DMA/60% PEG300/35% D5W, showed average (n = 2 mice) values of the maximum plasma concentration (C_{max}) of 285 ng/mL (1160 nM) and $AUC_{0\text{-}5h}$ of 547 h × ng/mL (Supplemental Information, Figure S1). Thus, the PK profile reinforced the needs for improving MIC and $t_{1/2}$, as a correlate of oral exposure in the mouse. With this in mind, we initiated the synthesis of a novel set of analogs of **JSF-3449** (Table 1).

As previous reports indicated that antitubercular activity is often associated with the 5-nitrofuran moiety,[11–14] we kept this moiety constant in our studies. We initially examined the linker length between the amide nitrogen and phenyl ring. Aniline **1**, phenethylamine **2**, and phenylpropylamine **3** were synthesized via a coupling reaction between the appropriate acid chloride and amine components, similar to that used to initially prepare **JSF-3449** (Scheme 1). It should be noted that **1** and **2** have been investigated previously by the Lee group in their studies of nitrofuranylamides and exhibited similar antitubercular activities as reported herein.[13] While the Vero cell cytotoxicity changed little with a linker length of 0 – 3 carbons, the trend for antitubercular efficacy followed: 1 > 3 > > 0 and 2 (Table 1).

Table 1
MIC and CC_{50} values of select nitrofuranylamides in μM.

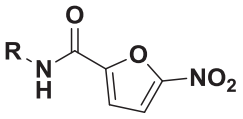

Compound	R	*M. tuberculosis* MIC (μM)	Vero Cell CC_{50} (μM)
JSF-3449	Benzyl	0.39	13
1	Phenyl	3.1	6.7
2	Phenethyl	3.1	12
3	Phenylpropyl	0.78	11
4	2-ClBenzyl	6.2	11
5	3-ClBenzyl	0.78	5.5
6	4-ClBenzyl	0.098	2.8
7	4-ClPhenyl	0.78	1.5
8	4-ClPhenethyl	0.39	5.4
9	4-ClPhenylpropyl	0.39	19

Next, we examined the effect of substituting the phenyl *ortho*-, *meta*-, or *para*-position in **JSF-3449** with a chlorine. The corresponding analogs, prepared according to the route for **JSF-3449** (Scheme 1), demonstrated divergent activity from the parent compound. 4-substituted compound **6** had a 4-fold enhancement in antibacterial activity (MIC = 0.098 μM), while 3-chloro compound **5** was twofold less potent and 2-substituted compound **4** lost 16x. Chloro substitution at any of the three positions of **JSF-3449** did lead to a reduction in the Vero cell CC_{50}, although the SI was only slightly decreased when translating from **JSF-3449** (SI = 33) to **6** (SI = 29). A return to the examination of the effect of tether length, while maintaining a 4-Cl phenyl moiety, demonstrated that the 0- (compound **7**), 2- (compound **8**), and 3-carbon spacers (compound **9**) afforded less potent compounds than the benzyl analog **6**. Analogs **9** and **8** did, however, offer reductions in the Vero cell cytotoxicity as compared to compound **6**.

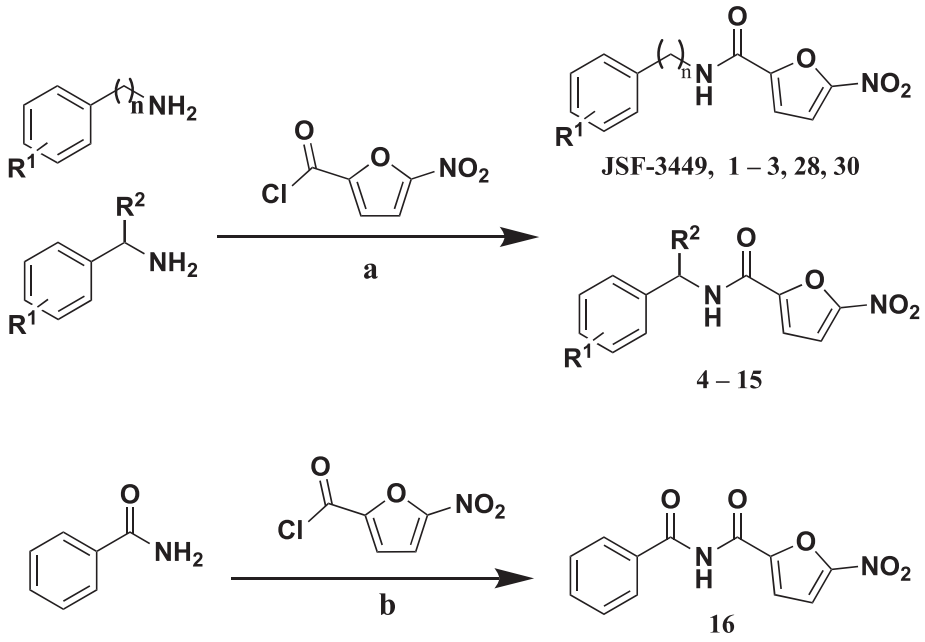

Scheme 1. Reagents and conditions: a) Et_3N, DCM; b) NaH, THF, 0 °C to rt.

Table 2
MIC and CC_{50} values of α-substituted nitrofuranylbenzylamides.

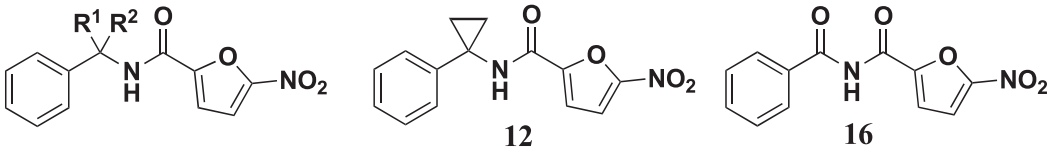

Compound	R^1	R^2	*M. tuberculosis* MIC (μM)	Vero Cell CC_{50} (μM)
JSF-3449	H	H	0.39	13
10	CH_3	H	6.2	24
11	CH_3	CH_3	0.78	> 180
12	CH_2[a]	CH_2[a]	6.2	46
13	Isopropyl	H	6.2	22
14	Cyclopropyl	H	12	22
15	*tert*-butyl	H	25	10
16	O	O	25	3.0

[a] Denotes a fused cyclopropyl ring to the benzylic carbon.

Subsequently, we sought to add different alkyl substituents to the benzylic carbon to reduce metabolic oxidation and, thus, improve MLM stability and mouse PK profile while potentially reducing cytotoxicity due to metabolite formation.[21] Returning to **JSF-3449** as the model compound, different groups were introduced at the benzylic carbon: methyl (compound **10**), α, α-dimethyl (compound **11**), a fused cyclopropyl (compound **12**), isopropyl (compound **13**), cyclopropyl (compound **14**), *tert*-butyl (compound **15**), and a carbonyl (compound **16**). The syntheses of these analogs were achieved following the routes in Scheme 1. All of the analogs, except α, α-dimethyl **11**, lost significant whole-cell activity (MIC = 6.2 – 25 μM) compared to **JSF-3449** (Table 2). **11** displayed a twofold increase in MIC compared to **JSF-3449**, but demonstrated a drastically improved CC_{50} of > 180 μM (SI > 230).

Compound **11** was profiled for *in vitro* MLM stability, aqueous solubility, and mouse PK (Table 3). In comparison to **JSF-3449**, **11** demonstrated enhanced $t_{1/2}$ (meeting the goal criteria) and mouse PK profile (Supplemental Information Figure S2) as judged by C_{max} and $AUC_{0\text{-}5h}$, although its S was depressed but still acceptable at 388 μM.

The α, α-dimethyl moiety was then held constant while the pendant aromatic ring was replaced with a subset of heterocycles. For example, benzothiophene (compound **17**), benzofuran (compound **18**), and 2-naphthalene (compound **19**) analogs were prepared following synthetic procedures depicted in Scheme 2, featuring the reductive dimethylation[22] of commercially available nitriles to afford the heterocyclic α, α-dimethylmethylamine for coupling with the 5-nitrofuroyl chloride. Replacement of phenyl with 2-naphthyl (**19**; MIC = 0.0078 μM), 2-benzothiophene (**17**; MIC = 0.078 μM), or 2-benzofuran (**18**; MIC = 0.20 μM) all afforded improvements in whole-cell activity (Table 4). While **17** and **18** displayed an increase in their Vero cell cytotoxicity compared to **11**, **19** did not exhibit significant cytotoxicity (CC_{50} > 150 μM). The mouse PK profiles for **19** and **17** showed very limited exposure in the plasma (Supplemental Information Figures S3 and S4, respectively). Their relative decreased metabolic stabilities (MLM $t_{1/2} \leq 2.13$ min) and S values may be responsible for this outcome.

We returned to the α, α-dimethyl benzylamide series and focused on the exploration of different substituents at the 4-position leveraging the synthetic route in Scheme 2. Analogs with an electron-donating group on the phenyl ring such as 4-*t*-butyl (compound **23**), 4-Me_2N

Table 3
MLM, solubility, and *in vivo* mouse PK (single 25 mg/kg dose po) profiles of **11** and **JSF-3449**.

Compound	MLM $t_{1/2}$ (min)	Cl_{int} (μL/min/mg protein)	Kinetic Solubility in pH 7.4 PBS (μM)	C_{max}[a] in ng/mL (nM)	$AUC_{0\text{-}5h}$[a] (h × ng/mL)
JSF-3449	28.5	24.3	> 500	285 (1160)	547
11	74.5	9.30	388	443 (1620)	717

[a] Average of two experiments.

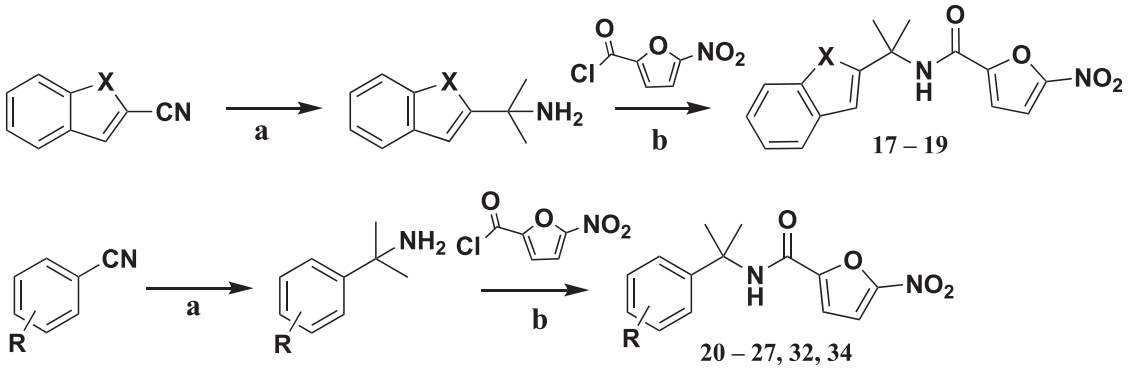

Scheme 2. Reagents and conditions: a) $CeCl_3$, CH_3Li, THF, −78 °C to rt; b) Et_3N, DCM.

Table 4
MIC and CC_{50} values of α, α-dimethylsubstituted nitrofuranylheteroarylamides.

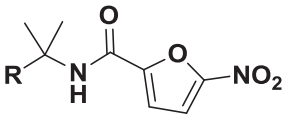

Compound	R	*M. tuberculosis* MIC (μM)	Vero Cell CC_{50} (μM)	MLM $t_{1/2}$ (min)	Cl_{int} (μL/min/mg protein)	Kinetic Solubility in pH 7.4 PBS (μM)
11	Phenyl	0.78	> 180	74.5	9.30	388
17	2-benzothiophene	0.078	38	1.87	371	5.61
18	2-benzofuran	0.20	40	n.d.	n.d.	n.d.
19	2-naphthyl	0.0078	> 150	2.13	325	1.50

n.d. = not determined.

Table 5
MIC and CC_{50} values of α, α-dimethyl substituted nitrofuranyl(4-substituted) benzylamides.

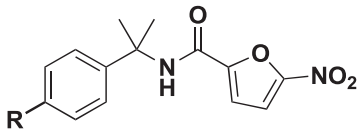

Compound	R	*M. tuberculosis* MIC (μM)	Vero Cell CC_{50} (μM)
11	H	0.78	> 180
20	4-Cl	0.15	81
21	4-OCH_3	0.078	82
22	4-Me_2N	0.20	79
23	4-*t*-Bu	0.39	> 150
24	4-OCF_3	0.20	70
25	4-F	0.78	42
26	4-CN	> 10	83
27	4-CF_3	0.78	> 150

(compound **22**), and 4-OCF_3 (compound **24**) were more active than **11**, but the 4-OCH_3 (**21**; MIC = 0.078 μM) analog was the most potent derivative (Table 5). In contrast, amongst compounds with electron-withdrawing moieties, only the 4-Cl analog (**20**; MIC = 0.15 μM) demonstrated an improvement in MIC over **11**. 4-F (compound **25**) and 4-CF_3 (compound **27**) analogs were equipotent to **11**, and the 4-CN (compound **26**) derivative failed to demonstrate significant activity (MIC > 10 μM). All but the 4-*t*-butyl (**23**) and 4-CF_3 (**27**) analogs exhibited a significant decrease in Vero cell cytotoxicity over **11**, although the SI values for 4-OCH_3 (**21**; SI = 1100) and 4-Cl (**20**; SI = 540) were

Table 6
MIC and CC_{50} values of nitrofuranyl(4-substituted)benzylamides in μM.

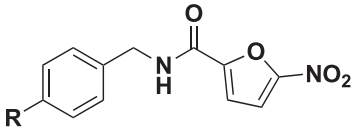

Compound	R	*M. tuberculosis* MIC (μM)	Vero Cell CC_{50} (μM)
28	4-chlorophenyl	0.12	4.4
29	4-chlorophenoxy	0.062	8.4
30	4-morpholinomethyl	1.2	18
31	4-chlorophenoxymethyl	0.039	4.0

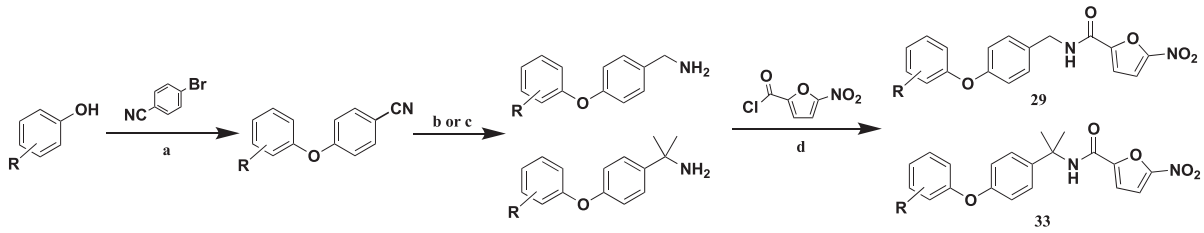

Scheme 3. Reagents and conditions: a) Cs_2CO_3, CuI, *N,N*-Dimethylglycine hydrochloride, dioxane, reflux, 24 h; b) Red-Al, THF, 0 °C to rt; c) $CeCl_3$, CH_3Li, THF, −78 °C to rt; d) Et_3N, DCM.

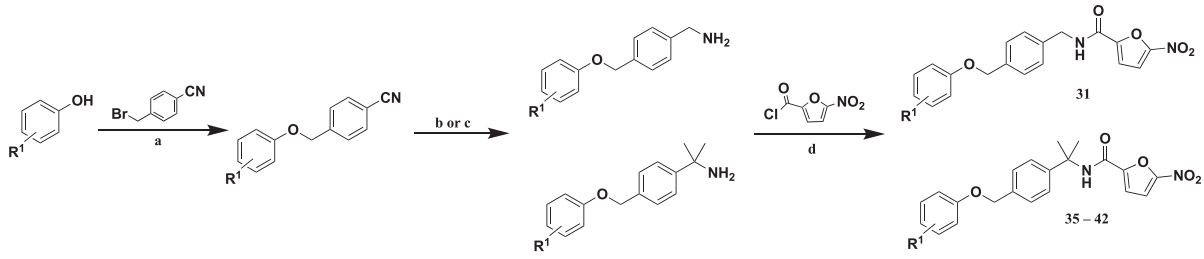

Scheme 4. Reagents and conditions: a) K_2CO_3, acetone, reflux, 48 h; b) Red-Al, THF, 0 °C to rt; c) $CeCl_3$, CH_3Li, THF, −78 °C to rt; d) Et_3N, DCM.

Table 7
MIC and CC_{50} values of α,α-disubstituted nitrofuranyl(4-substituted)benzylamides in μM.

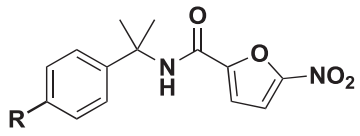

Compound	R	*M. tuberculosis* MIC (μM)	Vero Cell CC_{50} (μM)
11	H	0.78	> 180
32	4-chlorophenyl	25	> 140
33	4-chlorophenoxy	0.39	67
34	4-morpholinomethyl	> 10	130
35	4-chlorophenoxymethyl	0.12	120

Table 8
In vivo mouse PK (single 25 mg/kg dose po) profile of **11** and **35**.

Compound	C_{max}[a] in ng/mL (nM)	$AUC_{0\text{-}5h}$[a] (h × ng/mL)
11	443 (1620)	717
35	9.2 (22)	34

[a] Average of two experiments.

more than sufficient. Unfortunately, the mouse PK profile of **21** demonstrated low exposure in the plasma as compared to **11** (Supplemental Information, Figure S5).

The addition of larger substituents to the 4-position of the benzylamide ring was then pursued (Table 6). Returning for the moment to the methylene instead of α, α-dimethyl linker, we explored the following groups: 4-chlorophenyl (compound **28**), 4-chlorophenoxy (compound **29**), 4-morpholinomethyl (compound **30**), and 4-chlorophenoxymethyl (compound **31**). The analogs were synthesized according to the routes in Schemes 1, 3, and 4. The route in Scheme 3 depended on a copper(I)-catalyzed diaryl ether formation,[23] followed by reduction of the nitrile with Red-Al, and ended with amide formation via reaction with 5-nitrofuroyl chloride. The aromatic substituents afforded the more efficacious compounds: **31** (MIC = 0.039 μM), **29** (MIC = 0.062 μM), and **28** (MIC = 0.12 μM).

Table 9
MIC and CC_{50} values of α, α-dimethylsubstituted nitrofuranylbenzylamides in μM.

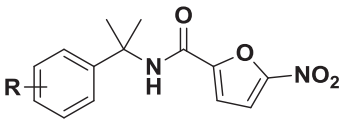

Compound	R	*M. tuberculosis* MIC (μM)	Vero Cell CC_{50} (μM)
35	4-chlorophenoxymethyl	0.12	120
36	4-methoxyphenoxymethyl	0.078	> 120
37	4-trifluoromethoxyphenoxymethyl	0.39	6.7
38	4-trifluoromethylphenoxymethyl	0.39	7.0
39	2-Chlorophenoxymethyl	0.31	30
40 (JSF-4088)	2-methoxyphenoxymethyl	0.019	> 120
41	2-trifluoromethoxyphenoxymethyl	0.098	13
42	2-trifluoromethylphenoxymethyl	0.31	14

In contrast, **30**, the morpholino analog, had modest antitubercular activity (MIC = 1.2 μM). We hypothesized that addition of a morpholine, as a solubilizing group, would help improve potency; however, this was not the case. All of these analogs displayed an increase in Vero cell cytotoxicity compared to **11**, although the SI values for **31** (SI = 100) and **29** (SI = 130) were sufficient.

Due to the potency of these analogs and having in mind to further improve Vero cell cytotoxicity, we synthesized their corresponding α, α-dimethyl analogs as depicted in Schemes 2, 3 and 4, featuring reduction[22] of the intermediate nitrile with $CeCl_3/CH_3Li$. Key intermediates in Scheme 4 were prepared by coupling the corresponding *meta*- or *para*-substituted phenol to 4-(bromomethyl) benzonitrile, using K_2CO_3 in refluxing acetone. All four analogs succeeded with respect to the goal of decreasing Vero cell cytotoxicity. 4-chlorobiphenyl (compound **32)** and 4-morpholinomethyl (compound **34**) showed significantly reduced antitubercular activity (MIC > 10 μM) towards *M. tuberculosis* (Table 7). In contrast, the 4-chlorophenoxy (compound **33**) and 4-chlorophenoxymethyl (compound **35**) analogs suffered more modest losses in antitubercular activity, displaying

Table 10
MLM, solubility, and *in vivo* mouse PK (single 25 mg/kg dose po) profiles of **11**, **36**, and **JSF-4088**.

Compound	MLM $t_{1/2}$ (min)	Cl_{int} (μL/min/mg protein)	Kinetic Solubility in pH 7.4 PBS (μM)	C_{max}[a] in ng/mL (nM)	$AUC_{0\text{-}5h}$[a] (h × ng/mL)
11	74.5	9.30	388	443 (1620)	717
36	45.0	15.4	< 0.06	BLQ[b]	11
JSF-4088	11.6	59.8	0.182	85 (210)	210

[a] Average of two experiments.
[b] Below limit of quantification of 5.0 ng/mL.

MIC values of 0.39 and 0.12 μM, respectively. In comparison to **11**, both **33** and **35** showed improved antitubercular activity. **35** demonstrated the best antitubercular activity with an excellent selectivity towards Vero cells (SI = 1000). **35** was, thus, profiled for mouse PK (Table 8). In comparison to **11, 35** showed much lower exposure as judged by C_{max} and $AUC_{0\text{-}5h}$ (Supplemental Information Figure S6).

Finally, further optimization around **35**, due to its increased *in vitro* potency over that of **11**, was proposed by adding different moieties such as OCH_3, OCF_3, and CF_3 in either the *meta*- or *para*-position of the terminal phenoxy ring. These analogs were synthesized following the route depicted in Scheme 4. As seen in Table 9, the 4-OCH_3 (compound **36**) analog showed improved antitubercular activity (MIC = 0.078 μM) compared to **35**, while maintaining low cytotoxicity (CC_{50} > 120 μM). Both the 4-OCF_3 (compound **37**) and 4-CF_3 (compound **38**) analogs were ca. 3-fold less potent than **35**, and showed relatively high Vero cell cytotoxicity. The 2-Cl (compound **39**) and 2-CF_3 (compound **42**) analogs exhibited similar sub-optimal profiles. 2-OCF_3 (compound **41**) was slightly more potent versus *M. tuberculosis* than **35**, but its CC_{50} was only 13 μM. 2-OCH_3 (compound **40**; **JSF-4088**) satisfyingly demonstrated improved potency (MIC = 0.019 μM) and Vero cell cytotoxicity (CC_{50} > 120 μM) than **35**.

As both **36** and **JSF-4088** showed improved antitubercular activity (in the absence of significant growth inhibition of the ESKAPE bacteria; Supplemental Information Table S1) over **35**, these two compounds were profiled for S, MLM $t_{1/2}$, and mouse PK (Table 10). **36** and **JSF-4088** did not improve upon the MLM stability or aqueous solubility of **11**, with the aqueous solubility of **36** being unacceptably low (≤ 0.06 μM). It was, therefore, not surprising, that plasma exposure of **36** was below the lower limit of quantification (LLOQ = 5.0 ng/mL). **JSF-4088** showed quantifiable absorption in the mice (Supplemental Information Figure S7), but still failed to improve upon the profile of **11**. In addition, it demonstrated poor accumulation in mouse lungs (mean C_{lung}/C_{plasma} = 0.06) at t = 5 h post administration of a single 25 mg/kg po dose (Supplemental Information, Table S2).

A family of novel *N*-benzyl-5-nitrofuran-2-carboxamides was designed and synthesized to optimize the hit compound **JSF-3449**. While addressing limitations in cytotoxicity and metabolic stability, the addition of an α, α-dimethyl moiety was a key modification. **11**, in particular, showed improved selectivity versus Vero cells (SI > 230), enhanced MLM stability ($t_{1/2}$ = 74.5 min), and enhanced mouse PK profile, while only demonstrating small setbacks with regard to MIC and S. Further SAR optimization of **11** led to **JSF-4088** with significantly improved *in vitro* potency (MIC = 0.019 μM) and Vero cell cytotoxicity window (SI > 6300). However, **JSF-4088** was unable to improve upon the still modest mouse PK profile of **11**. Further PK profile optimization remains as a challenge to this series of compounds with outstanding *in vitro* potency against *M. tuberculosis*. This challenge may be answered by merging our use of α, α-dimethyl substitution of the benzylic carbon in conjunction with a broader range of substitutions of the pendant phenyl moiety as exemplified in reports of nitrofuranyl amides by Tangallapally et al.,[13,15] which despite generally being less potent *in vitro* versus *M. tuberculosis* and more cytotoxic to Vero cell cultures did display *in vivo* efficacy in an interferon-γ knockout mouse model of infection.

Acknowledgements

The authors gratefully acknowledge support from NIH grants R33AI11167, R21AI111647, and U19AI109713.

Appendix A. Supplementary data

Supplementary data to this article can be found online at https://doi.org/10.1016/j.bmcl.2018.12.053.

References

1. World Health Organization. *Global Tuberculosis Report.* 2017.
2. Shah NS, Auld SC, Brust JC, et al. Transmission of Extensively Drug-Resistant Tuberculosis in South Africa. *N Engl J Med.* 2017;376(3):243–253.
3. Stover CK, Warrener P, VanDevanter DR, et al. A small-molecule nitroimidazopyran drug candidate for the treatment of tuberculosis. *Nature.* 2000;405:962–966.
4. Matsumoto M, Hashizume H, Tomishige T, et al. OPC-67683, a nitro-dihydro-imidazooxazole derivative with promising action against tuberculosis in vitro and in mice. *PLoS Med.* 2006;3:2131–2144.
5. Wayne LG, Sramek HA. Metronidazole Is bactericidal to dormant cells of *Mycobacterium tuberculosis*. *Antimicrob Agents Chemother.* 1994;38:2054–2058.
6. Carroll MW, Jeon D, Mountz JM, et al. Efficacy and safety of metronidazole for pulmonary multidrug-resistant tuberculosis. *Antimicrob Agents Chemother.* 2013;57(8):3903–3909.
7. Manjunatha UH, Boshoff H, Dowd CS, et al. Identification of a nitroimidazo-oxazine-specific protein involved in PA-824 resistance in *Mycobacterium tuberculosis*. *Proc Natl Acad Sci.* 2006;103:431–436.
8. Singh R, Manjunatha U, Boshoff HI, et al. PA-824 kills nonreplicating Mycobacterium tuberculosis by intracellular NO release. *Science.* 2008;322(5906):1392–1395.
9. Bloemberg GV, Keller PM, Stucki D, et al. Acquired Resistance to Bedaquiline and Delamanid in Therapy for Tuberculosis. *N Engl J Med.* 2015;373(20):1986–1988.
10. Haver HL, Chua A, Ghode P, et al. Mutations in genes for the F420 biosynthetic pathway and a nitroreductase enzyme are the primary resistance determinants in spontaneous in vitro-selected PA-824-resistant mutants of Mycobacterium tuberculosis. *Antimicrob Agents Chemother.* 2015;59(9):5316–5323.
11. Fan YL, Wu JB, Ke X, Huang ZP. Design, synthesis and evaluation of oxime-functionalized nitrofuranylamides as novel antitubercular agents. *Bioorg Med Chem Lett.* 2018;28(18):3064–3066.
12. Hurdle JG, Lee RB, Budha NR, et al. A microbiological assessment of novel nitrofuranylamides as anti-tuberculosis agents. *J Antimicrob Chemother.* 2008;62(5):1037–1045.
13. Tangallapally RP, Yendapally R, Lee RE, et al. Synthesis and evaluation of nitrofuranylamides as novel antituberculosis agents. *J Med Chem.* 2004;47(21):5276–5283.
14. Yempalla KR, Munagala G, Singh S, et al. Nitrofuranyl Methyl Piperazines as New Anti-TB Agents: Identification, Validation, Medicinal Chemistry, and PK Studies. *ACS Med Chem Lett.* 2015;6(10):1041–1046.
15. Tangallapally RP, Yendapally R, Lee RE, Lenaerts AJ, Lee RE. Synthesis and evaluation of cyclic secondary amine substituted phenyl and benzyl nitrofuranyl amides as novel antituberculosis agents. *J Med Chem.* 2005;48(26):8261–8269.
16. Rakesh Bruhn DF, Scherman MS, et al. Pentacyclic nitrofurans with in vivo efficacy and activity against nonreplicating Mycobacterium tuberculosis. *PLoS ONE.* 2014;9(2)::e87909.
17. Ekins S, Reynolds RC, Kim H, et al. Bayesian models leveraging bioactivity and cytotoxicity information for drug discovery. *Chem Biol.* 2013;20:370–378.
18. Inoyama D, Paget SD, Russo R, Novel,, et al. Pyrimidines as Antitubercular Agents. *Antimicrob Agents Chemother.* 2018;62(3)..
19. Wilson R, Kumar P, Parashar V, et al. Antituberculosis thiophenes define a requirement for Pks13 in mycolic acid biosynthesis. *Nat Chem Biol.* 2013;9(8):499–506.
20. Rusan M, Petrovanu O. Leonte C. In vitro antimicrobial effect of some benzylamine and thienylamine derivatives. *Analele Stiintifice ale Universitatii AI I Cuza din Iasi, Sectiunea 1c Chimie.* 1967;13(2):153–156.
21. Talele TT. Natural-Products-Inspired Use of the gem-Dimethyl Group in Medicinal Chemistry. *J Med Chem.* 2018;61(6):2166–2210.
22. Ciganek E. Tertiary carbinamines by addition of organocerium reagents to nitriles and ketimines. *J Org Chem.* 1992;57:4521–4527.
23. Ma D, Cai Q. N, N-dimethyl glycine-promoted Ullmann coupling reaction of phenols and aryl halides. *Org Lett.* 2003;5(21):3799–3802.